Selectivity in Gas-Phase Ion Chemistry. Competitive Fast Reactions in a Silane/Propene System

Carlo Canepa,* Andrea Maranzana, Lorenza Operti,* Roberto Rabezzana, and Gian Angelo Vaglio

Dipartimento di Chimica Generale ed Organica Applicata, Università degli Studi di Torino, Corso Massimo d'Azeglio 48, 10125 Torino, Italy

Received April 24, 2001

Gas-phase selective reactions have been studied in silane/propene mixtures by ion-trap mass spectrometry and density functional calculations. Products from the third step of reaction of SiH^+ ions with SiH_4 and C_3H_6 were selected and reacted in the cell of a quadrupole ion trap. The prior steps have been the subject of a previous study by this research group. While ions $Si_3H_5^+$, $Si_4H_7^+$, and $Si_mC_nH_p^+$ react selectively with propene, collisions with silane do not lead to any detectable product besides self-condensation of silane. Experimental and collisional rate constants of the main processes have been compared, determining reaction efficiencies. Chain propagation proceeds until the formation of large clusters, such as $Si_2C_5H_{13}^+$, $Si_3C_2H_n^+$ ($n = 9, 11$), and $Si_4C_2H_{11}^+$, is attained. The critical points on the B3LYP/6-311G(d,p) potential energy surfaces of the $Si_2H_3^+/C_3H_6$ and $Si_3H_5^+/C_3H_6$ systems have been found, describing the structures of the most stable reaction products. The observed selectivity toward propene of species $Si_2CH_5^+$ and $Si_3CH_7^+$ with respect to two alternative reaction channels (silane or propene) is explained in terms of relative reaction entropies of the corresponding adducts.

1. Introduction

Both fundamental and applied studies of gas-phase reactions between ion species and neutral molecules are attracting increasing interest,[1] as in chemical vapor deposition of thin films by ion clusters from ion/molecule reactions in activated gaseous mixtures.[2] While the reactivity in condensed phases is usually affected by ion pairing and solvation interactions, gas-phase studies allow exploitation of the intrinsic reactivity of charged species.[3] Of prominent relevance is information on mechanisms of clustering reactions and determination of rate constants for the initial chain propagation steps. In fact, this knowledge can direct the choice of experimental conditions aimed toward optimizing abundances of the appropriate ion species affording amorphous solids of the desired composition and properties.[4] Theoretical studies complement experimental findings and improve knowledge of mechanistic details, as structures of intermediates and products, reaction energy profiles, and thermodynamical data.[2a,5]

In the past, both experimental investigations on mechanisms and kinetics of self-condensation reactions of SiH_4 and complementary quantum chemistry calculations have been reported.[5c,d] In particular, mixtures of SiH_4 and hydrocarbons have been studied under high-pressure conditions[6] and recently investigated in our laboratory by ion-trap mass spectrometry.[5p,7] These systems become suitable starting reagents in the chemical vapor deposition of amorphous silicon carbides after

* Corresponding authors. Fax: 39 011 670 7591. E-mail: canepa@ch.unito.it and operti@ch.unito.it.

(1) (a) Cacace F. *Pure Appl. Chem*. **1997**, *69*, 227−229. (b) Schroeder, D.; Heineman, C.; Koch, W.; Schwarz, H. *Pure Appl. Chem*. **1997**, *69*, 273−280. (c) Speranza, M. *Trends Organomet. Chem*. **1994**, *1*, 35−62. (d) Goldberg, N.; Schwarz, H. In *The Chemistry of Organic Silicon Compounds*; Rappoport, Z., Apeloig, Y., Eds.; Wiley: Chichester, 1998; Vol. 2, pp 1105−1142. (e) Gronert S. *Chem. Rev*. **2001**, *101*, 329−360.

(2) (a) Jackson, P.; Srinivas, R.; Langermann, N.; Diefenbach, M.; Schroeder, D., Schwarz, H. *Int. J. Mass Spectrom*. **2000**, *201*, 23−40. (b) Antoniotti, P.; Benzi, P.; Castiglioni, M.; Volpe, P. *Eur. J. Inorg. Chem*. **1999**, 323−332.

(3) (a) Bowers, M. T.; Marshall, A. G.; Mclafferty, F. W. *J. Phys. Chem*. **1996**, *100*, 12897−12910. (b) Nibbering, N. M. M. *Int. J. Mass Spectrom*. **2000**, *200*, 27−42.

(4) (a) Gal, J. F.; Grover; R., Maria, P. C.; Operti, L.; Rabezzana, R.; Vaglio, G. A.; Volpe, P. *J. Phys. Chem*. **1994**, *98*, 11978−11987. (b) Antoniotti, P.; Operti, L.; Rabezzana, R.; Vaglio, G. A.; Volpe, P.; Gal, J. F.; Grover, R.; Maria, P. C. *J. Phys. Chem*. **1996**, *100*, 155−162. (c) Benzi, P.; Operti, L.; Rabezzana, R. *Eur. J. Inorg. Chem*. **2000**, 505−512.

(5) (a) Wlodeck, S.; Fox, A.; Bohme, D. K. *J Am. Chem. Soc*. **1991**, *113*, 4461−4468. (b) Srinivas, R.; Hrusak, J.; Sulzle, D.; Bohme, D. K.; Schwarz, H. *J. Am. Chem. Soc*. **1992**, *114*, 2802−2806. (c) Reents, W. D., Jr.; Mandich, M. L. *J Chem. Phys*. **1992**, *96*, 4429−4439. (d) Raghavachari, K. *J. Chem. Phys*. **1992**, *96*, 4440−4448. (e) Cipollini, R.; Crestoni, M. E.; Fornarini, S. *J. Am. Chem. Soc*. **1997**, *119*, 9499−9503. (f) Chiavarino, B.; Crestoni, M. E.; Di Rienzo, B.; Fornarini, S. *J. Am. Chem. Soc*. **1998**, *120*, 10856−10862. (g) Antoniotti, P.; Operti, L.; Rabezzana, R.; Splendore, M.; Tonachini, G.; Vaglio, G. A. *J. Chem. Phys*. **1997**, *107*, 1491−1500. (h) Antoniotti, P.; Operti, L.; Rabezzana, R.; Tonachini, G.; Vaglio, G. A. *J. Chem. Phys*. **1998**, *109*, 10853−10863. (i) Antoniotti, P.; Operti, L.; Rabezzana, R.; Tonachini, G.; Vaglio, G. A. *J. Chem. Phys*. **2000**, *112*, 1814−1822. (j) Cruz, E. M.; Lopez, X.; Ayerbe, M.; Ugalde, J. M. *J. Phys. Chem*. **1997**, *101*, 2166−2172. (k) Bernardi, F.; Cacace, F.; de Petris, G.; Pepi, F.; Rossi, I. *J. Phys. Chem. A* **1998**, *102*, 1987−1994. (l) Bernardi, F.; Cacace, F.; de Petris, G.; Pepi, F.; Rossi, I. *J. Phys. Chem. A* **1998**, *102*, 5831−5836. (m) Karni, M.; Apeloig, Y.; Schroeder, D.; Zummack, W.; Rabezzana, R.; Schwarz, H. *Ang. Chem., Int. Ed*. **1999**, *38*, 331−335. (n) Jackson, P.; Diefenbach, M.; Schroeder, D.; Schwarz, H. *Eur. J. Inorg. Chem*. **1999**, 1203−1210. (o) Jackson P.; Sandig N.; Diefenbach M.; Schroeder D.; Schwarz, H.; Srinivas R. *Chem. Eur. J*. **2001**, *7*, 151−160. (p) Antoniotti, P.; Canepa, C.; Operti, L.; Rabezzana, R.; Tonachini, G.; Vaglio, G. A. *J. Phys. Chem. A* **1999**, *103*, 10945−10954. (q) Antoniotti, P.; Canepa, C.; Maranzana, A.; Operti, L.; Rabezzana, R.; Tonachini, G.; Vaglio, G. A. *Organometallics* **2001**, *20*, 382−391.

(6) (a) Mayer, T. M.; Lampe, F. W. *J. Phys. Chem*. **1974**, *78*, 2433−2437. (b) Allen, W. N.; Lampe, F. W. *J. Am. Chem. Soc.* **1977**, *99*, 6816−6822.

10.1021/om010339+ CCC: $20.00
Publication on Web 10/05/2001

the appropriate activation by laser, X-ray, or other methods. The high efficiency of mixed ions $Si_mC_nH_p^+$ toward C_3H_6 (rather than SiH_4) is a remarkable feature of the ion chemistry of this system. While reaction mechanisms and rate constants of the initial kinetic steps leading to the formation of silicon and carbon-containing ion clusters in silane/propene mixtures have previously been published,[7a] this work extends the experimental investigation to later steps of the polymerization.

The significant selectivity displayed by these systems prompted us to investigate further, and we report in this paper experimental results on reaction channels leading to ion clusters of larger size. We set our goal to establish if trends of the initial reaction steps described in ref 7a are also followed in the ensuing chain propagation paths. Theoretical analyses explore the relevant reaction pathways and single out the dominant factors determining the high selectivity never before observed in gas-phase processes in mixtures of silane or germane with hydrocarbons.

2. Experimental Section

2.1. Materials. Silane (99.997% purity) and propene (99.99%) were supplied by SIAD. The SiH_4/C_3H_6 mixture was prepared in the ion-trap cell by connection of the flasks to the gas inlet system. Helium buffer gas was purchased from SIAD at the extrahigh purity of 99.9999%.

2.2. Mass Spectrometry. All experiments have been performed on an ITMS Finnigan mass spectrometer. Gas pressures were measured with a Bayard Alpert ionization gauge and corrected accounting for the relative sensitivity of the ion gauge to different gases.[8] Pressures were also corrected by an additional calibration factor, as previously reported.[9] Helium was introduced into the trap at a pressure of $\sim 4 \times 10^{-4}$ Torr (1 Torr = 133 Pa). The trap temperature was set at 333 K, as in previous studies of related systems. The manifold and lines for the introduction of reactant gases were baked frequently to prevent side reactions with the background water. In all experiments ions were detected in the 14−300 u mass range. Scan modes used to determine reaction mechanisms have previously been described in detail, as well as procedures for the calculation of rate constants.[4b,5g,9] Samples are ionized by impact with an electron beam at ~35 eV. A time lag after the ionization event maximizes relative intensities of ions under examination and is followed by isolation of the selected ions, their storage in the trap for convenient reaction times, and their acquisition.

The single exponential decays observed in kinetic experiments are consistent with the hypothesis that reactant ions eliminate most of their excitation energy through collisions.

2.3. Methods of Calculation. Quantum chemistry calculations were carried out using the Gaussian98 suite of programs[10] utilizing gradient geometry optimization.[11] All structures were fully optimized at the B3LYP level of theory.[12] The 6-311G(d,p) basis set has been used throughout the study. Vibrational frequency calculations were used to characterize the stationary points as either minima or first-order saddle points at the level indicated. Molecular structures have been plotted with the program Moldraw.[13]

3. Results and Discussion

3.1. Mass Spectrometry. The first three reaction steps of ion/molecule reactions in silane/propene mixtures have been investigated in a previous paper.[7a] The observed formation of ions containing both Si and C (mixed ions) mainly takes place through reactions with propene as the neutral reactant. Selectivity toward propene was also observed for all the charged species in the reaction sequences originated from SiH_n^+ (n = 0−3) primary ions; however SiH^+ displayed the highest yield in clustering processes. Therefore, its chain propagation has been considered in this work, selecting and reacting the products of the third reaction step, until the abundances of ions allowed collection of reproducible results. These reaction mechanisms are summarized in Scheme 1, where the reactions previously investigated are reported above the dashed line.

Mixed ion species studied experimentally in this work react selectively with propene, yielding clusters of increasing size, whereas no product of reaction with molecules of silane has been observed. Figure 1 shows an example of this behavior, with mass spectra recorded 40 ms after isolation and reaction of $SiC_2H_7^+$ (a), $Si_3CH_7^+$ (b), and $Si_2C_3H_7^+$ (c) in the 1:1 silane/propene mixture. All reacting ions exhibit the addition of C_3H_6 and the loss of ethene as the most common reaction pathway. In a parallel step, $Si_2C_2H_7^+$, $Si_2C_3H_9^+$, and $Si_3CH_7^+$ also react with the loss of an ethyne molecule. The chain propagation of $Si_2C_2H_7^+$ through three consecutive steps is also followed by formation of the large cluster $Si_2C_5H_{13}^+$.

Experimental rate constants of the above processes, collisional rate constants, and reaction efficiencies are reported in Table 1. Processes listed in Table 1 are generally slower with respect to the first reaction steps, but most are fast enough to afford appreciable intensities of product ions. It is worth noting that the addition of a CH_2 moiety (C_2H_4 elimination) is always faster than the corresponding addition of a CH_4 fragment (C_2H_2 elimination). Reliable rate constants for the formation of reaction products could not always be determined due to the low abundance of the ions involved.

The selectivity of mixed species toward propene was quite intriguing, and a theoretical study has been

(7) (a) Antoniotti, P.; Operti, L.; Rabezzana, R.; Vaglio, G. A.; Volpe, P. *Int. J. Mass Spectrom.* **1999**, *190/191*, 243−251. (b) Antoniotti, P.; Canepa, C.; Operti, L.; Rabezzana, R.; Tonachini, G.; Vaglio, G. A. *J. Organomet. Chem.* **1999**, *589*, 150−156.

(8) (a) Decouzon, M.; Gal, J.-F.; Maria, P.-C.; TchInianga, A. S. Personal communication. (b) Bartmess, J. E.; Georgiadis, R. M. *Vacuum* **1983**, *33*, 149.

(9) Operti, L.; Splendore, M.; Vaglio, G. A.; Franklin, A. M.; Todd, J. F. J. *Int. J. Mass Spectrom. Ion Processes* **1994**, *136*, 25−33.

(10) Frisch, M. J.; Trucks, G. W.; Schlegel, H. B.; Scuseria, G. E.; Robb, M. A.; Cheeseman, J. R.; Zakrzewski, V. G.; Montgomery, J. A., Jr.; Stratmann, R. E.; Burant, J. C.; Dapprich, S.; Millam, J. M.; Daniels, A. D.; Kudin, K. N.; Strain, M. C.; Farkas, O.; Tomasi, J.; Barone, V.; Cossi, M.; Cammi, R.; Mennucci, B.; Pomelli, C.; Adamo, C.; Clifford, S.; Ochterski, J.; Petersson, G. A.; Ayala, P. Y.; Cui, Q.; Morokuma, K.; Malick, D. K.; Rabuck, A. D.; Raghavachari, K.; Foresman, J. B.; Cioslowski, J.; Ortiz, J. V.; Baboul, A. G.; Stefanov, B. B.; Liu, G.; Liashenko, A.; Piskorz, P.; Komaromi, I.; Gomperts, R.; Martin, R. L.; Fox, D. J.; Keith, T.; Al-Laham, M. A.; Peng, C. Y.; Nanayakkara, A.; Gonzalez, C.; Challacombe, M.; Gill, P. M. W.; Johnson, B.; Chen, W.; Wong, M. W.; Andres, J. L.; Gonzalez, C.; Head-Gordon, M.; Replogle, E. S.; Pople, J. A. *Gaussian98*; Gaussian, Inc.: Pittsburgh, PA, 1998.

(11) Gonzalez, C.; Schlegel, H. B. *J. Chem. Phys.* **1989**, *90*, 2154.

(12) (a) Becke, A. D. *J. Chem. Phys.* **1993**, *98*, 5648. (b) Stevens, P. J.; Devlin, F. J.; Chablowski, C. F.; Frisch, M. J. *J. Phys. Chem.* **1994**, *80*, 11623.

(13) (a) Ugliengo, P.; Viterbo, D.; Borzani, G. *J. Appl. Crystallogr.* **1988**, *21*, 75. (b) Ugliengo, P.; Borzani, G.; Viterbo, D. *Z. Crystallogr.* **1988**, *185*, 712. (c) Ugliengo, P.; Viterbo, D.; Chiari, G. *Z. Crystallogr.* **1993**, *207*, 9.

Scheme 1

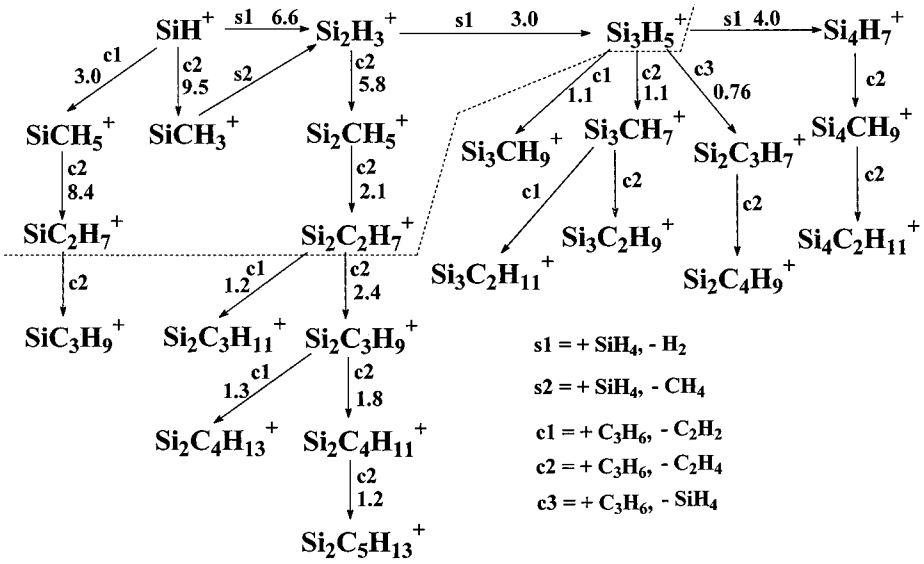

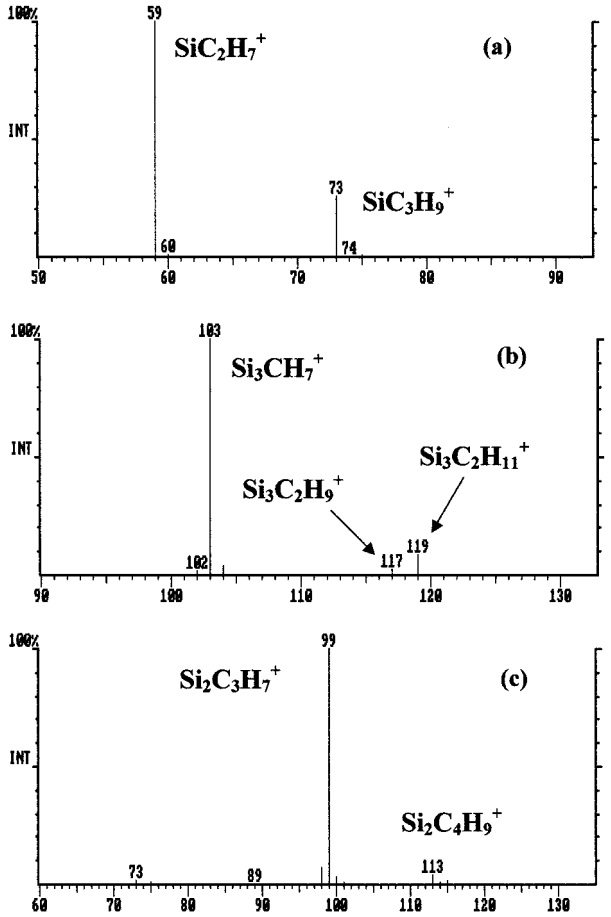

Figure 1. Mass spectra of the 1:1 SiH_4/C_3H_6 mixture after 40 ms of reaction of the $SiC_2H_7^+$ (a), $Si_3CH_7^+$ (b), and $Si_2C_3H_7^+$ (c) selectively isolated ions.

undertaken to investigate the thermodynamical features of these reactions. To this purpose, the reaction mechanisms starting from $Si_2H_3^+$ and $Si_3H_5^+$ have been studied by density functional calculations.

3.2. Theoretical Study. 3.2.1. Reaction of $Si_2H_3^+$ with Propene. The first step of the overall sequence of gas-phase reactions of $Si_2H_3^+$ leading to the mixed ion clusters $Si_mC_nH_p^+$ is schematically summarized in reaction I. The secondary ion $Si_2CH_5^+$ and ethene are formed through the adduct species $Si_2C_3H_9^+$, not observed experimentally.

$$Si_2H_3^+ \textbf{(1)} + C_3H_6 \textbf{(2)} \rightarrow Si_2C_3H_9^+ \textbf{(3–9)} \rightarrow C_2H_4 \textbf{(10)} + Si_2CH_5^+ \textbf{(11–14)} \quad \text{(I)}$$

In a subsequent step the cation $Si_2CH_5^+$ further reacts selectively with propene (reaction II) to give $Si_2C_2H_7^+$ and C_2H_4 through the adduct $Si_2C_4H_{11}^+$ (**15**). No charged product of reaction with silane (**16**, reaction III) through the $Si_3CH_9^+$ adduct (**17**) is observed. Both adducts **15** and **17** are not detected experimentally.

$$Si_2CH_5^+ \textbf{(12)} + C_3H_6 \textbf{(2)} \rightarrow Si_2C_4H_{11}^+ \textbf{(15)} \rightarrow Si_2C_2H_7^+ + C_2H_4 \quad \text{(II)}$$

$$Si_2CH_5^+ \textbf{(12)} + SiH_4 \textbf{(16)} \rightarrow Si_3CH_9^+ \textbf{(17)} \quad \text{(III)}$$

A theoretical study of the first polymerization steps provides insight into the favored formation of $Si_2C_4H_{11}^+$ (reaction II) with respect to $Si_3CH_9^+$ (reaction III).

(a) Step I. The ion–molecule interaction of tribridged cation **1** (its potential energy surface has been described by Raghavachari,[14] Köhler, and Lischka[15]) with propene (**2**) forms the adduct **3**, 25.95 kcal mol^{-1} below isolated reactants (Figure 2). Both Si atoms in **1** interact with the three hydrogens. The π system of propene in species **3** bridges unsymmetrically to Si, at 2.221 and 2.094 Å, respectively. Correspondingly, this interaction elongates the double bond of propene by 0.072 Å.

The virtual absence of a barrier for the subsequent hydrogen shift from the methyl group of propene to the bridging Si atom in TS-**4** suggests that formation of ion **5** (Figure 3) is a very fast process that leads to a structure with a HSi–SiH_3 group symmetrically interacting with an allyl moiety. This interaction lowers the potential energy (including the zero-point contribution, ΔU_{ZPE}) to −49.95 kcal mol^{-1} with respect to isolated

(14) Raghavachari, K. *J. Chem. Phys.* **1991**, *95*, 7373.
(15) Köhler, H. J.; Lischka, H. *Chem. Phys. Lett.* **1984**, *112*, 33.

Table 1. Rate Constants for Reactions of $SiC_2H_7^+$, $Si_2C_2H_7^+$, $Si_2C_3H_9^+$, $Si_2C_4H_{11}^+$, and $Si_3H_5^+$ with Propene in Silane/Propene Mixtures[a]

ion	products ions (rate constants, k_{exp})	Σk_{exp}	$k_{collisional}$[b]	efficiency[c]
$SiC_2H_7^+$	$SiC_3H_9^+$ (4.8)	4.8	12.51	0.38
$Si_2C_2H_7^+$	$Si_2C_3H_9^+$ (2.4), $Si_2C_3H_{11}^+$ (1.2)	3.6	11.61	0.31
$Si_2C_3H_9^+$	$Si_2C_4H_{11}^+$ (1.8), $Si_2C_4H_{13}^+$ (1.3)	3.1	11.35	0.27
$Si_2C_4H_{11}^+$	$Si_2C_5H_{13}^+$ (1.2)	1.2	11.14	0.11
$Si_3H_5^+$	$Si_2C_3H_7^+$ (0.76), $Si_3CH_7^+$ (1.1), $Si_3CH_9^+$ (1.1)	3.0	11.60	0.26

[a] Rate constants are expressed as 10^{-10} cm^3 molecule^{-1} s^{-1}; uncertainty is within 20%. [b] Collisional rate constants have been calculated according to the ADO theory taking the polarizabilty (6.26×10^{-24} cm^3) and dipole moment (0.366 D) of propene from: Maryott, A. A.; Buckley, F. U.S. National Bureau of Standards Circular No. 537, 1953. [c] Efficiency has been calculated as the ratio $k_{exp}/k_{collisional}$.

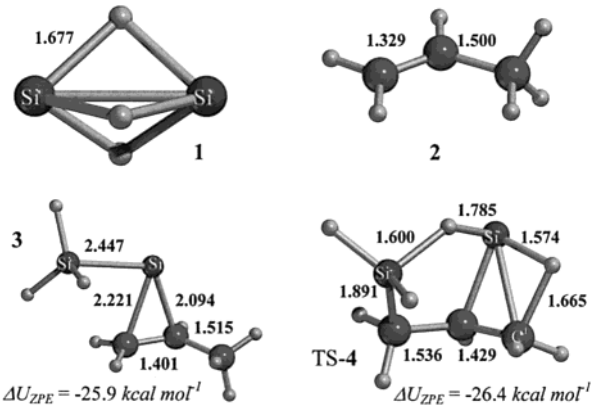

Figure 2. Isolated reactants $Si_2H_3^+$ (**1**) and C_3H_6 (**2**), their adduct (**3**), and the transition structure for hydrogen transfer from propene to the Si_2H_3 moiety (TS-**4**). Geometries are optimized at the B3LYP/6-311G(d,p) level, distances are in Å.

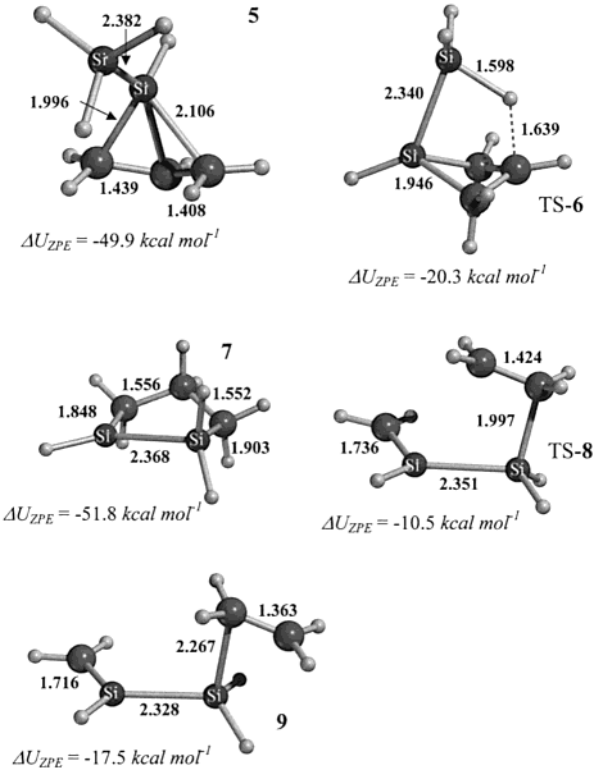

Figure 3. Isomers of adduct $Si_2C_3H_9^+$ (**5**, **7**, **9**) and the transition structures for cyclization (TS-**6**) and ring opening (TS-**8**). Geometries are optimized at the B3LYP/6-311G-(d,p) level, distances are in Å.

reactants. The migrating hydrogen is at 1.665 Å from C^1 and at 1.574 Å from Si^5 in TS-**4**, where the Si−Si bond is disrupted and both Si atoms are connected to the same hydrogen. The Si−Si bond is restored in minimum **5** (Figure 3).

Table 2. Energies with Zero-Point Correction (ΔU_{ZPE}, kcal mol^{-1}) Relative to Isolated Reactants (Singlet $Si_2H_3^+$ and C_3H_6) of Transition Structures, Intermediates, and Products ($Si_2CH_5^+$ and C_2H_4)[a]

species	ΔU_{ZPE}	species	ΔU_{ZPE}
1 + **2**	0.00	**10** + **11**	3.51
3	−25.95	**10** + **12**	−4.91
TS-**4**	−26.38	**10** + **13**	0.98
5	−49.95	**10** + **14**	11.06
TS-**6**	−20.27		
7	−51.81		
TS-**8**	−10.54		
9	−17.54		

[a] Energies are computed at the B3LYP/6-311G(d,p) level of theory.

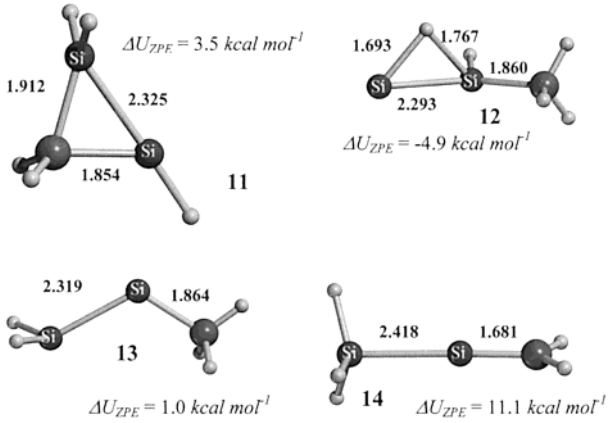

Figure 4. Products $Si_2CH_5^+$ (**11**−**14**). Geometries are optimized at the B3LYP/6-311G(d,p) level, distances are in Å.

In the following step along the reaction coordinate one hydrogen atom from the SiH_3 group shifts to the central allyl carbon in TS-**6**, 20.27 kcal mol^{-1} below isolated reactants. The resulting closed structure **7** represents the most stable isomer with formula $Si_2C_3H_9^+$. Its difference in potential energy with respect to isolated reactant is −51.81 kcal mol^{-1}. The vibrationally excited **7** leads, through TS-**8**, to the open-chain ion **9** at −17.54 kcal mol^{-1}. Table 2 summarizes the differences in potential energy of species **1** + **2** through **9**. Cleavage of the H_2Si-CH_2 bond in **9** gives the kinetic products C_2H_4 (**10**) and **11** at 3.51 kcal mol^{-1} (Figure 4). Compound **11** can thermally rearrange to the more stable structure **12** (ΔU_{ZPE} = −4.91 kcal mol^{-1}), bridging one hydrogen between the two Si atoms. Two other isomers of higher energy (**13**, **14**, Table 3) are also reported in Figure 4.

(b) Step II and III. To determine which of the competitive processes II and III is favored, geometries

Table 3. Energies with Zero-Point Correction (ΔU_{ZPE}, kcal mol^{-1}) Relative to Isolated Reactants (Singlet $Si_3H_5^+$ and C_3H_6) of Transition Structures, Intermediates, and Products ($Si_3CH_7^+$ and C_2H_4)[a]

species	ΔU_{ZPE}	species	ΔU_{ZPE}
2 + **18**	0.00	**10** + **26**	3.81
19	−23.71	**10** + **27**	−7.70
TS-**20**	−23.71		
21	−46.98		
TS-**22**	−18.39		
23	−49.65		
TS-**24**	−11.09		
25	−15.59		

[a] Energies are computed at the B3LYP/6-311G(*d*,*p*) level of theory.

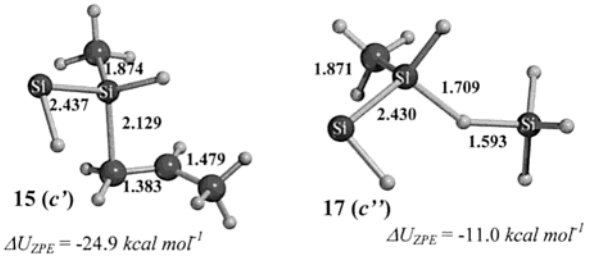

Figure 5. Adducts of **12** with C_3H_6 (**15**, *c*′) and SiH_4 (**17**, *c*″). Geometries are optimized at the B3LYP/6-311G(d,p) level, distances are in Å. Energies are relative to the isolated reactants propene + **12** and SiH_4 + **12**.

of clusters **15** and **17** have been optimized (Figure 5). Both are below the potential energy of the corresponding isolated reactants **12** and propene/silane (ΔU_{ZPE} = −24.89 and −10.97 kcal mol^{-1}, respectively). The silicon atom linked to CH_3 in adduct **15** binds at 2.129 Å the terminal C atom of propene. In **17** the cation $Si_2CH_5^+$ coordinates a hydrogen atom of SiH_4 at 1.709 Å, with a weaker binding energy of −11.0 kcal mol^{-1}.

3.2.2. Reaction of $Si_3H_5^+$ with Propene. The reaction of $Si_3H_5^+$ with propene follows a pathway similar to the lighter ion $Si_2H_3^+$, forming $Si_3CH_7^+$ and ethene through the adduct ion $Si_2C_4H_{11}^+$, never observed experimentally (reaction IV).

$$Si_3H_5^+ \textbf{(18)} + C_3H_6 \textbf{(2)} \rightarrow Si_3C_3H_{11}^+ \textbf{(19}-\textbf{25)} \rightarrow C_2H_4 \textbf{(10)} + Si_3CH_7^+ \textbf{(26, 27)} \quad \text{(IV)}$$

Product ions $Si_3CH_7^+$ react selectively in a subsequent step with propene through the adduct $Si_3C_4H_{13}^+$ in reaction V, whereas the competitive process with silane (reaction VI) does not take place.

$$Si_3CH_7^+ \textbf{(27)} + C_3H_6 \textbf{(2)} \rightarrow Si_3C_4H_{13}^+ \textbf{(28)} \rightarrow Si_3C_2H_9^+ + C_2H_4 \quad \text{(V)}$$

$$Si_3CH_7^+ \textbf{(26)} + SiH_4 \textbf{(16)} \rightarrow Si_4CH_{11}^+ \textbf{(29)} \quad \text{(VI)}$$

(a) Step IV. Cation **18** binds to propene in the bridged structure **19** (Figure 6), at −23.71 kcal mol^{-1} with respect to isolated reactants. Two subsequent fast hydrogen shifts (TS-**20** and TS-**22**) afford complex **21** and cycle **23**, at −49.65 kcal mol^{-1} (Figure 7). Ring **23** has thus enough vibrational energy to open via TS-**24** to compound **25**, where an ethene molecule bridges its π system to the $Si_3CH_7^+$ cation (Figure 7, Table 3). Separating the two fragments of cluster **25** yields the

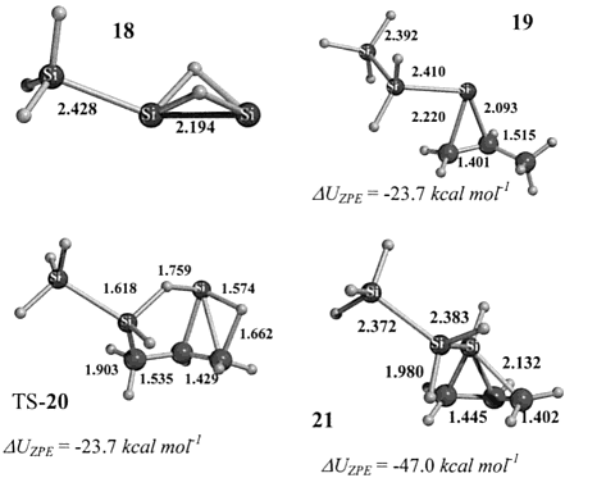

Figure 6. Reactant $Si_3H_5^+$ and its adduct with C_3H_6 (**19**), the transition structure for hydrogen transfer from propene to the Si_3H_5 moiety (TS-**20**), and the isomer of adduct $Si_3C_3H_{11}^+$ (**21**). Geometries are optimized at the B3LYP/6-311G(d,p) level, distances are in Å.

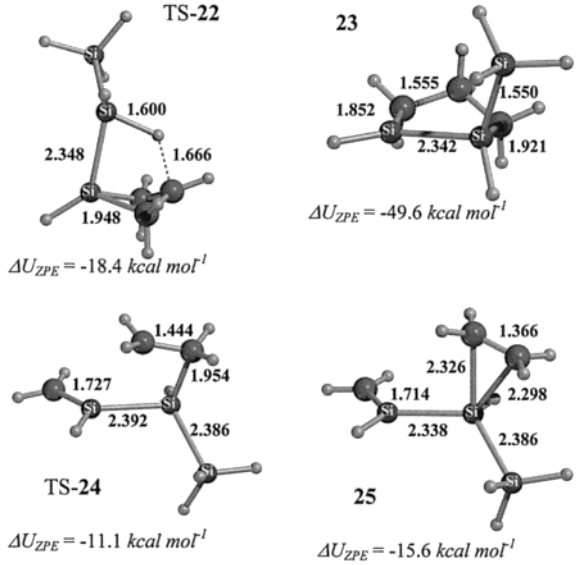

Figure 7. Isomers of adduct $Si_3C_3H_{11}^+$ (**23**, **25**) and the transition structures for cyclization (TS-**22**) and ring opening (**TS-24**). Geometries are optimized at the B3LYP/6-311G(d,p) level, distances are in Å.

kinetic product **26** at 3.81 kcal mol^{-1} (19.40 kcal mol^{-1} above **25**), which in turn thermically rearranges to the more stable **27** (−7.70 kcal mol^{-1}, Figure 8, Table 3).

(b) Steps V and VI. In principle, product **27** is able to bind to both propene and silane, as already seen for compound **12**. Through adducts **28** and **29**, whose geometries have been optimized, the two competitive processes (Figure 8, Table 3) may propagate the polymer increasing either its carbon or silicon content. In the following section we estimate the relative entropies of processes II versus III and V versus VI.

3.2.3. Competitive Clustering of Cations with Silane or Propene. A silicon-containing cation *a*, formed by the consecutive reaction I or IV, can in principle react further either with propene (*b*′) or silane (*b*″), in the competitive processes.

$$a + b' \rightarrow c' \quad (1)$$

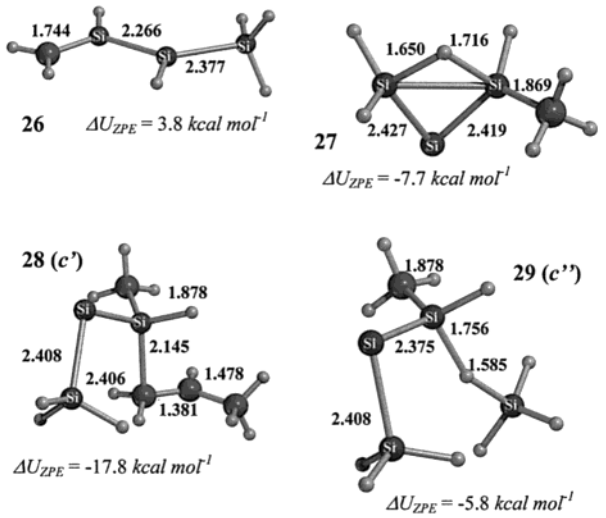

Figure 8. Isomers of product $Si_3CH_7^+$ (**26**, **27**) and adducts of **27** with C_3H_6 (**28**, *c*′) and SiH_4 (**29**, *c*″). Geometries are optimized at the B3LYP/6-311G(d,p) level, distances are in Å.

$$a + b'' \rightarrow c'' \tag{2}$$

We want to determine which is actually favored. Since the experiments described in this paper were carried out at low concentrations of neutral reactants (ca. 10^{-9} mol·L^{-1}), the lifetime of complexes *c*′ and *c*″ is much shorter than the average time between collisions with the buffer gas.[16] In the virtual absence of collisions, the energy accumulated in the adduct complex cannot be equilibrated, and systems such as **15**, **17**, **28**, and **29** may be considered isolated. Therefore, their absolute entropies with respect to reactants $a + b$ must be used as criteria for their formation. To compute the difference in entropy between product and reactants (ΔS) in reactions 1 and 2, first we note that the total energy is conserved in the collision between species *a* and *b*. We may write the conservation of energy as

$$E_a(T_0) + E_b(T_0) - \Delta U = E_t(T_t) + E_r(T_r) + E_v(T_v) \tag{3}$$

In the above equation E_x indicates the sum of translational, rotational, and vibrational energy of species *x* and ΔU the binding energy of the product cluster. The reacting species are thermalized at temperature T_0. We can define the effective translational, rotational, and vibrational temperatures of the cluster after the collision: T_t, T_r, T_v, respectively. The total entropy of the species *c* may be expressed in terms of the effective temperatures

$$S(T_t,T_r,T_v) = S_t(T_t) + S_r(T_r) + S_v(T_v), \tag{4}$$

where T_t, T_r, and T_v are in turn determined by the energy of the corresponding contribution. In principle we do not know how the total energy will be distributed among E_t, E_r, and E_v. Consequently, we can only calculate the effective vibrational temperature T_v for each possible outcome of the translational energy $E_t = (3/2)kT_t$, in the assumption that the rotational energy before and after the collision has the average value $(3/2)kT_0$. Equation 3 takes the form

$$\frac{9}{2}NkT_0 + NkT_0{}^2\left[\frac{(\partial_T z_{v(a)}(T_0))_V}{z_{v(a)}(T_0)} + \frac{(\partial_T z_{v(b)}(T_0))_V}{z_{v(b)}(T_0)}\right] - \Delta U - E_t - E_v(T_v) = 0 \tag{5}$$

where $\partial_x \equiv \partial/\partial x$.

Equation 5 has been solved for $T_v(E_t)$ and the solution used in eq 4. We can thus write in eq 6 the total entropy of the cluster as a function of its translational energy:

$$S(E_t) = Nk \ln\left(\frac{4\pi m E_t}{3h^2}\right)^{3/2}\frac{V}{N}e^{5/2} + S_r(T_0) + S_v[T_v(E_t)] \tag{6}$$

The rotational and vibrational contribution to the total entropy are expressed in terms of the corresponding partition functions[17] as

$$S_r(T_0) = Nk\left(\ln z_r(T_0) + T_0\frac{(\partial_T z_r(T_0))_V}{z_r(T_0)}\right) \tag{7}$$

and

$$S_v[T_v(E_t)] = Nk\left(\ln z_v(T_v) + T_v\frac{(\partial_T z_v(T_v))_V}{z_v(T_v)}\right) \tag{8}$$

where

$$z_r = \frac{1}{\sigma}\left(\frac{\pi T^3}{\theta_{r,1}\theta_{r,2}\theta_{r,3}}\right)^{1/2} \tag{9}$$

$$(\partial_T z_r)_V = \frac{3}{2}\frac{z_r}{T}, \tag{10}$$

$$z_v = \prod_{j=1}^{3n-6}\frac{e^{-\theta_{v,j}/2T}}{1 - e^{-\theta_{v,j}/T}} \tag{11}$$

and

$$(\partial_T z_v)_V = \frac{z_v}{2T^2}\sum_{j=1}^{3n-6}\theta_{v,j}\frac{1 + e^{-\theta_{v,j}/T}}{1 - e^{-\theta_{v,j}/T}}. \tag{12}$$

The quantities θ_r and θ_v in eqs 9 and 11 represent the rotational and vibrational temperatures, respectively. All partition functions have been evaluated in the rigid rotor−harmonic oscillator approximation.

The effective vibrational temperatures of clusters with lower potential energy with respect to isolated reactants are considerably higher than the temperature of the colliding fragments (Tables 4 and 5). This is also shown in Figure 9a, where the effective temperatures of clusters of type *c*′ (**15**, **28**) and *c*″ (**17**, **29**) are plotted as functions of their translational energies.

The differences $S_{c'} - S_{c''}$ for clusters **15**, **17**, and **28**, **29** are reported in Figure 9b as functions of the corresponding translational energies. The total entropy of clusters *c*′ is always in excess with respect to clusters *c*″ by more than 20 cal mol^{-1} K^{-1}. This result supports the formation of the adduct with a propene molecule as

(16) (a) Aschi, M.; Attinà, M.; Cacace, F.; D'Arcangelo, G. *J. Am. Chem. Soc.* **1998**, *120*, 3982−3987. (b) Aschi, M.; Attinà, M.; Cacace, F. *Chem. Eur. J.* **1998**, *4*, 1535−1541. (c) De Puy, C. H. *Int. J. Mass Spectrom.* **2000**, *200*, 79−96.

(17) McQuarrie, D. A. *Statistical Thermodynamics*; University Science Books: Mill Valley, CA, 1973; pp 133−136.

Table 4. Electronic Energy Differences (ΔU, kcal mol^{-1}) and Effective Vibrational Temperatures (T_v, K) of Clusters Formed by Singlet $Si_2CH_5^+$ (12) with C_3H_6 (2) and SiH_4 (16) at 333 K[a]

species	ΔU	T_v	ΔT[b]
2 + **12**	0.00	333	
15	−27.36	844	511
16 + **12**	0.00	333	
17	−13.10	640	307

[a] Results are computed at the B3LYP/6-311G(d,p) level of theory, assuming $E_t = (3/4)kT_0(1 + 2\mu)$ and $E_r = (3/2)kT_0$ for species **15** and **17**. [b] ΔT represents the difference in temperature between products **15** and **17** with respect to isolated reactants at 333 K.

Table 5. Electronic Energy Differences (ΔU, kcal mol^{-1}) and Effective Vibrational Temperatures (T_v, K) of Clusters Formed by Singlet $Si_3CH_7^+$ (27) with C_3H_6 (2) and SiH_4 (16) at 333 K[a]

species	ΔU	T_v	ΔT[b]
2 + **27**	0.00	333	
28	−19.06	641	308
16 + **27**	0.00	333	
29	−6.48	448	115

[a] Results are computed at the B3LYP/6-311G(d,p) level of theory assuming $E_t = (3/4)kT_0(1 + 2\mu)$ and $E_r = (3/2)kT_0$ for species **28** and **29**. [b] ΔT represents the difference in temperature between products **28** and **29** with respect to isolated reactants at 333 K.

always more favorable than the corresponding formation of the adduct with silane.

4. Conclusions

This investigation of gas-phase ion/molecule reactions in silane/propene mixtures shows the complementarity of experimental and theoretical methods to understand the reactivity in gaseous systems. Formation of $Si_mC_nH_p^+$ cluster ions, possible precursors of amorphous silicon carbides, occurs through selective reactions of propene with $Si_xH_y^+$ charged species, from self-condensation of SiH_4, or with lighter silicon- and carbon-containing ions. This selectivity was observed in the first three reaction steps of primary ions of silane and has been confirmed here up to the sixth reaction step. The high entropy of the adducts formed in reactions with propene molecules as neutrals is responsible for the selectivity in the ion/molecule reactions of this system. Absolute entropies and effective temperatures of adducts from two competitive reaction channels were calculated from molecular partition functions. The favored products exhibit the largest entropies and temperatures, both significantly increased with respect to the thermalized reacting fragments.

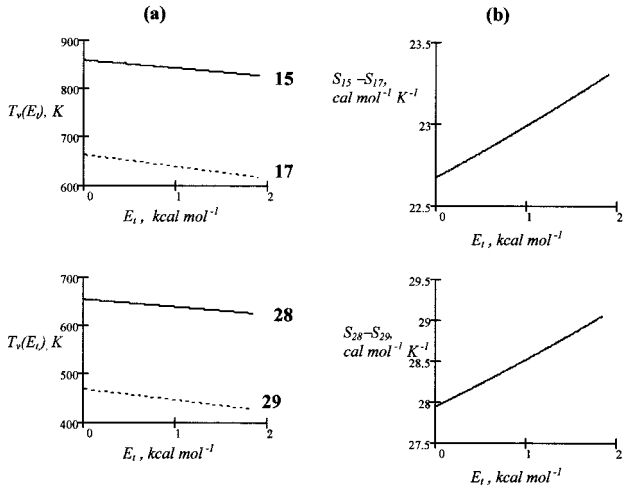

Figure 9. (a) Effective vibrational temperature (T_v) of clusters of type *c′* (**15** and **28**, $Si_mCH_n^+ \cdot C_3H_6$) and of type *c″* (**17** and **29**, $Si_mCH_n^+ \cdot SiH_4$) ($m = 2, 3$; $n = 5, 7$) and (b) their difference in entropy as a function of kinetic energy (E_t). The data have been computed assuming $E_r = (3/2)kT_0$.

Acknowledgment. Financial support was provided in part by the Italian MURST and Università degli Studi di Torino through the "Cofinanziamento di Programmi di Ricerca di Rilevante Interesse Nazionale", within the project "Chimica in Fase Gassosa di Specie Reattive Neutre e Cariche". C. Canepa thanks Prof. R. D. Bach for a helpful discussion.

OM010339+